

Determination of gamma-ray parameters for polyethylene glycol of different molecular weights

Ibrahim F. Al-Hamarneh^{1,2} · Mohammad W. Marashdeh² · Fahad I. Almasoud^{3,4} · Ahmad Alkaoud²

Received: 27 October 2016/Revised: 13 February 2017/Accepted: 13 February 2017/Published online: 25 October 2017
© Shanghai Institute of Applied Physics, Chinese Academy of Sciences, Chinese Nuclear Society, Science Press China and Springer Nature Singapore Pte Ltd. 2017

Abstract Mass attenuation coefficient (μ_m) for polyethylene glycol (PEG) of different molecular weights was determined by using NaI (TI) scintillator and WinXcom mixture rule at gamma energies of 59.5, 302.9, 356.0, 661.7, 1173.2 and 1332.5 keV. The total atomic, molecular and electronic cross sections, half-value layer, effective atomic and electron numbers, mass energy-absorption coefficients and kerma relative to air are calculated. The energy and compositional dependence of μ_m values, and the related radiation absorption parameters, are evaluated and discussed. The experimental results agree well with the theoretical ones, within an uncertainty of 1% in the effective atomic number for all PEG samples at the designated energies.

Keywords Polyethylene glycol · Mass attenuation coefficient · Effective atomic number · Electron density · Kerma relative to air

The authors thank the Deanship of Scientific Research at Al Imam Mohammad Ibn Saud Islamic University for the grant and financial assistance to accomplish this work.

✉ Ibrahim F. Al-Hamarneh
hamarnehibrahim@gmail.com

¹ Department of Physics, Faculty of Science, Al-Balqa Applied University, Al-Salt 19117, Jordan

² Department of Physics, College of Science, Al Imam Mohammad Ibn Saud Islamic University (IMSIU), Riyadh 11623, Saudi Arabia

³ Nuclear Science Research Institute, King Abdulaziz City for Science and Technology (KACST), Riyadh 11442, Saudi Arabia

⁴ National Centre for Nuclear Technology (NCNT), King Abdulaziz City for Science and Technology (KACST), Riyadh 11442, Saudi Arabia

1 Introduction

Polyethylene glycol (PEG), a polymer composed of the $-\text{CH}_2-\text{CH}_2-\text{O}-$ repeating units, is one of the most widely synthetic and inexpensive materials that have medical, chemical, biological and industrial uses [1–4]. PEG of different molecular weights is commercially available and is well known as non-toxic, non-immunogenic, amphiphatic and biocompatible polymers. PEG is utilized as a polymer–protein conjugate [5] and also known for its ability to mitigate protein adsorption and cell adhesion [1]. Thus, it has been successfully attached to biomedical implants, joint replacements and tissue substitutes [6–9]. Besides, it is effective for biochips and biosensors [10], medical instruments and implants technology [11]. With its distinctive physical properties, PEG is chosen for this investigation because it may play an important role in developing radiation shielding and phantom technologies, medical and nuclear applications, and radiation dosimeters. Therefore, knowledge of PEG molecules' radiological parameters, such as mass attenuation and mass energy-absorption coefficients, interaction cross sections, effective atomic numbers, half-value layer and kerma, is vital for understanding their physical properties. In the same context, knowledge of gamma-ray interaction with PEG is essential for radiation and nuclear physics and chemistry, radiation protection and dosimetry, and biomedical and technological fields [12–16].

A great number of authors reported the mass attenuation coefficients and related parameters for a variety of materials, including dosimeters, metals, polymers, and biological and medical materials [17–25], but none of the works were dedicated to evaluating the gamma attenuation performance of PEG. Therefore, it is important to study the

radiation protection capabilities of this particular polymer against gamma irradiation [26]. To achieve this, an investigation of the behavior and performance of PEG of different molecular weights against different gamma rays has been carried out.

PEG of molecular different weights provides a scope for various applications. For example, PEG molecular weight (chain length) affects the long-term stability of biomedical applications and the biofouling performance of PEG [27]. The chain length of PEG is a crucial factor affecting its grafting density, the number of hydrogen bonds and other properties of PEG [28]. On the other hand, PEG of low molecular weights was significantly effective as a hydrate inhibitor for designing drilling fluids [29]. It is thus of interest to identify the photon energy-absorption parameters of PEG of various molecular weights.

In this research, the mass attenuation coefficients (μ_m) for five PEG products were measured at 59.5, 302.9, 356.0, 661.7, 1173.2 and 1332.5 keV by using NaI (TI) scintillator, and were calculated by using mixture rule. Total atomic, molecular and electronic cross sections (σ_a , σ_m and σ_e), half-value layer (HVL), effective atomic and electron numbers (Z_{eff} and N_{eff}), mass energy-absorption coefficients and kerma relative to air for the PEG samples were calculated. These radiation interaction data are not tabulated in the literatures but are widely used in the shielding and dosimetry calculations used for medical diagnostic, therapeutic procedures and radiation biophysics. Therefore, the results can hopefully facilitate the use of PEG in specific applications such as gamma-ray shielding effectiveness, phantom technology and many others.

2 Experimental

PEG of molecular weights of 1000, 10,000, 20,000, 100,000 and 200,000 was obtained from Sigma-Aldrich (Germany). The common name, molecular formula, molecular weight and mean atomic number of each PEG sample are given in Table 1. The mean atomic number was calculated as: $\langle Z \rangle = \sum f_i Z_i$, where Z_i is the atomic

Table 1 Conventional names (CN), molecular formula (MF), molecular weights (MW) and mean atomic numbers $\langle Z \rangle$ of the PEG polymers

CN	MF	MW (Daltons)	$\langle Z \rangle$
PEG 1000	C ₄₄ H ₉₀ O ₂₃	987.17	3.4268
PEG 10,000	C ₄₅₄ H ₉₁₀ O ₂₂₈	10,017.95	3.4284
PEG 20,000	C ₉₀₈ H ₁₈₁₈ O ₄₅₅	20,017.88	3.4285
PEG 100,000	C ₄₅₄₀ H ₉₀₈₂ O ₂₂₇₁	100,017.33	3.4286
PEG 200,000	C ₉₀₈₀ H ₁₈₁₆₂ O ₄₅₄₁	200,016.64	3.4286

number of the i th element, $f_i = n_i / \sum n_i = n_i / n$ is the fractional abundance of the i th element with respect to the number of atoms in the compound, n_i is the number of formula units of the i th constituent element in the compound and n is the total number of atoms in the molecule.

Each PEG sample was compressed in hydraulic press to thin disk of $\Phi 1 \text{ cm} \times 0.2 \text{ cm}$. The PEG samples were exposed to gamma rays from four standard point sources (10 mCi) of ^{214}Am (59.5 keV), ^{133}Ba (302.9 and 356.0 keV), ^{137}Cs (661.7 keV) and ^{60}Co (1173.2 and 1332.5 keV). A $\Phi 2'' \times 2''$ NaI (TI) scintillation detector (EG&G Ortec, USA) was used. The source–detector distance was 25 cm (Fig. 1), and the detector energy resolution was 8% at 662 keV. A gamma spectrum was collected with a 2048-channel MCA, in data collection time of 3000 s to ensure good statistics. The gamma spectra were analyzed using the Maestro-ORTEC. Each sample was measured for three times, and the average value was taken for calculating the parameters. The gamma-ray absorption of PEG samples was evaluated by a narrow beam collimated by two lead collimators of a $\Phi 5\text{-mm}$ aperture [30]: one in front of the source and the other above the detector (Fig. 1). PEG samples in mass thicknesses of 0.21–0.47 g/cm^2 were positioned at 15 cm from the source.

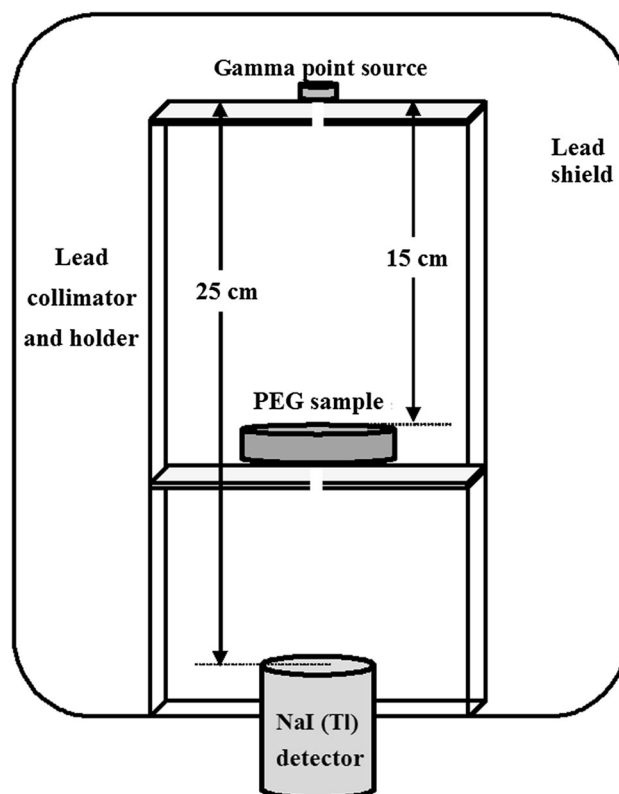


Fig. 1 Experimental setup for measuring γ -ray attenuation of PEG samples

The μ_m for different PEG samples and energies was calculated by Eq. (1) [31]:

$$I = I_0 e^{-\mu_m x}, \tag{1}$$

where I_0 and I denote the incoming and attenuated photon intensities, respectively; μ_m (cm^2/g) = μ_ℓ/ρ , with μ_ℓ (cm^{-1}) being the linear attenuation coefficient; ρ (g/cm^3) is the mass density; and x (g/cm^2) is mass thickness of the sample. For a material composed of more than one element, μ_m is calculated by WinXcom [32] based on the mixture rule [33] as:

$$\mu_m = \sum_i w_i (\mu_m)_i, \tag{2}$$

where $(\mu_m)_i$ is μ_m of the i th element in the composite and $w_i = n_i A_i / \sum n_j A_j$ is the proportion by weight of the i th element, where A_i is the atomic weight of that element. The mixture rule gives the attenuation coefficients of any substance as the sum of the appropriately weighted contributions from the individual atoms. The WinXcom can generate cross sections or attenuation coefficients on a standard energy grid, spaced approximately logarithmically, on a grid specified by the user, or for a mix of both grids. This program provides total cross sections and attenuation coefficients as well as partial cross sections for incoherent and coherent scattering, photoelectric absorption and pair production [34].

The maximum uncertainties ($\Delta\mu_m$) in μ_m coefficients were calculated by Eq. (3):

$$\Delta\mu_m = \frac{1}{x} \sqrt{\left(\frac{\Delta I_0}{I_0}\right)^2 + \left(\frac{\Delta I}{I}\right)^2 + \left(\ln \frac{I_0}{I}\right)^2 \left(\frac{\Delta x}{x}\right)^2}, \tag{3}$$

where ΔI_0 , ΔI and Δx are the uncertainties in the intensities I_0 and I and the mass thickness x , respectively. For composite materials, the effective atomic number (Z_{eff}) is used to describe the gamma-ray interaction processes [35, 36], calculated by [39]:

$$Z_{\text{eff}} = \sigma_a / \sigma_e, \tag{4}$$

where σ_a is the atomic cross section [37] and σ_e is the total electronic cross section [38]:

$$\sigma_a = \frac{1}{N_A} \sum_i f_i A_i (\mu_m)_i = \frac{\mu_m A_r}{N_A}, \tag{5}$$

$$\sigma_e = \frac{1}{N_A} \sum_i \frac{f_i A_i (\mu_m)_i}{Z_i}. \tag{6}$$

The mass attenuation coefficient is used to calculate the total molecular cross section (σ_m):

$$\sigma_m = \frac{\mu_m M}{N_A} = n \sigma_a, \tag{7}$$

where $M = \sum n_i A_i$ is the molecular weight of the compound. The effective electron number is calculated as:

$$N_{\text{eff}} = \frac{N_A}{N} Z_{\text{eff}} \sum_i n_i = \frac{(\mu_m)_{\text{polymer}}}{\sigma_e}, \tag{8}$$

where N_A is the Avogadro's number and $A_r = \sum n_i A_i / \sum n_i = M/n$ is the relative atomic mass of the compound.

The half-value layer, the material width required to reduce the air kerma of an X- or γ -ray to half its value, is defined as: $HVL = \ln 2 / \mu_\ell$. $\tag{9}$

Kerma (kinetic energy released per unit mass) in a material is feasible to uncharged particles and photons and is related to energy fluence and mass energy-absorption coefficient (μ_{en}/ρ). Kerma of PEG material relative to air is calculated as:

$$\text{Kerma} = (\mu_{\text{en}}/\rho)_{\text{PEG}} / (\mu_{\text{en}}/\rho)_{\text{air}}, \tag{10}$$

where the $(\mu_{\text{en}}/\rho) = \sum w_j (\mu_{\text{en}}/\rho)_j$ for PEG or air [40, 41]. For air, the $(\mu_{\text{en}}/\rho)_i$ coefficients are taken from Ref. [42].

3 Results and discussions

The μ_m values for PEG 100,000 measured and calculated at the selected photon energies are shown in Fig. 2, while the inset shows μ_m values for the other PEG samples. Experimental uncertainty in μ_m coefficient was estimated at $\leq 3\%$, being mainly due to uncertainty in measuring the mass density and thickness, and counting the incident and transmitted gamma intensities. The μ_m depends evidently on the photon energy and the chemical composition of

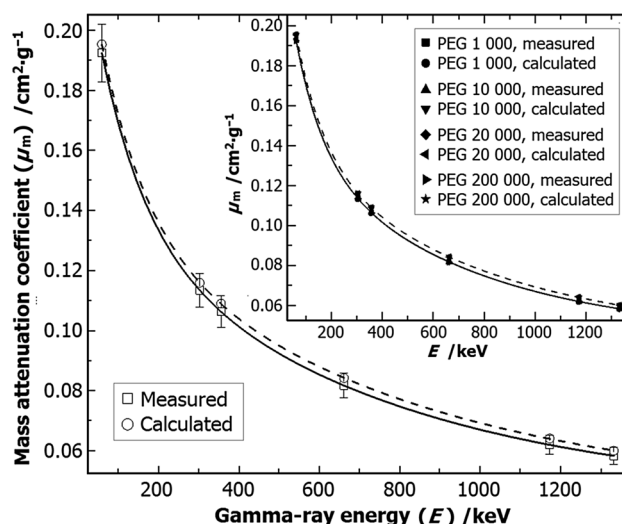


Fig. 2 μ_m values versus photon energy for PEG 100,000. The inset shows the μ_m for other PEG samples. The confidence level is 95%

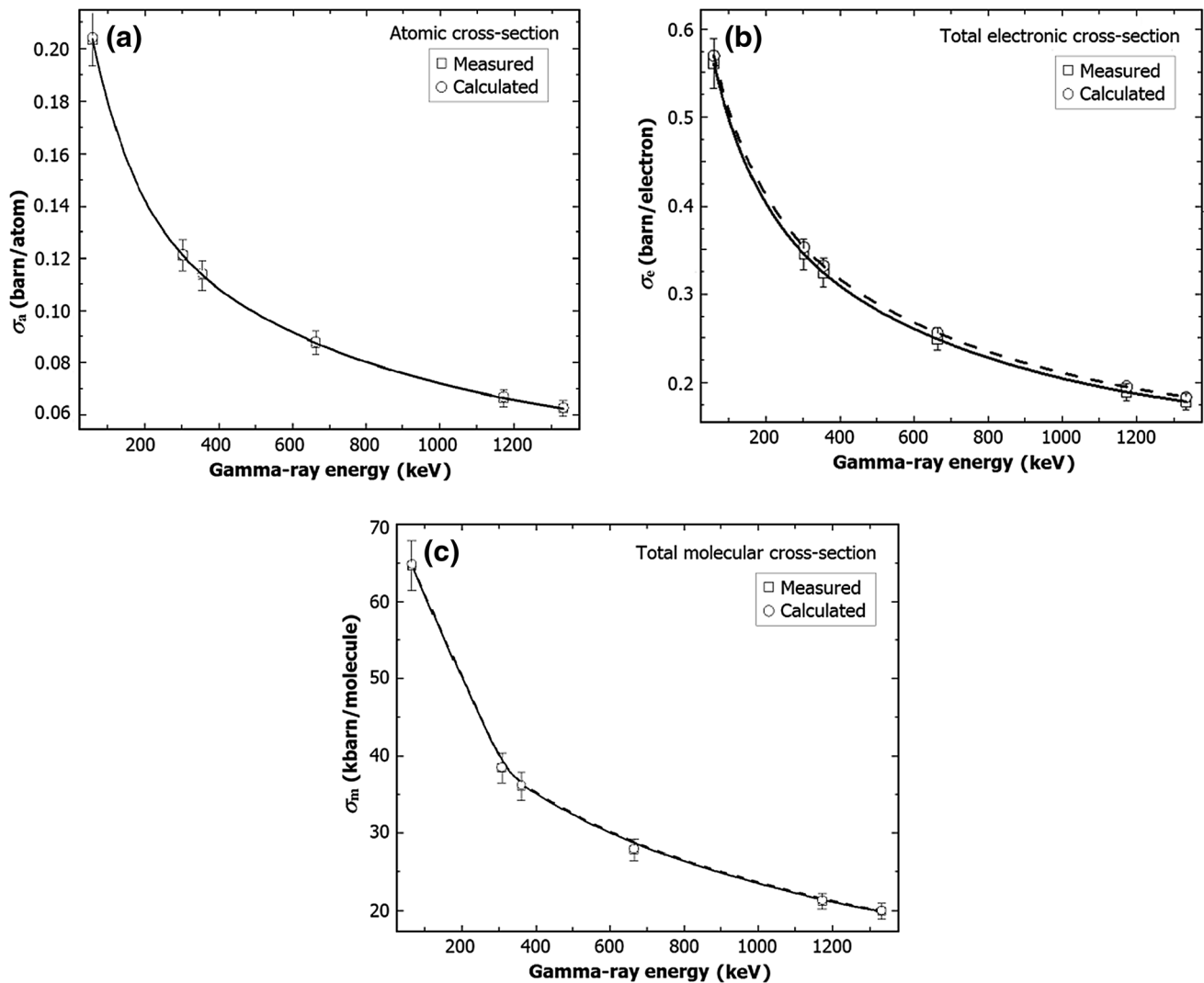


Fig. 3 a–c σ_a , σ_e and σ_m versus photon energy for sample PEG 200,000. Uncertainty bars indicate the 95% confidence level

PEG. At low energy region, the μ_m coefficient decreases sharply with increasing energy, as photoelectric absorption is the main interaction between gamma rays and PEG, which is characterized by the importance of atomic binding. Compton scattering process at intermediate energies (302.9, 356.0 and 661.7 keV), and pair production process at high energies (1173.2 and 1332.5 keV), dominates over photoelectric absorption process. Thus, μ_m coefficients show a less energy-dependent behavior and gradual decrease with increasing energy. Figure 2 and its inset show that the measured μ_m for almost all samples is slightly lower than the calculated values. However, they agree well with each other within the experimental uncertainty. The observed discrepancy between measured and calculated values of μ_m may be ascribed to potential existence of trace amounts of impurities in the PEG materials. Other factors may include possible deviation of

the experimental setup from perfect-narrowness, causing systematic uncertainty in the measured values of μ_m [43].

The σ_a , σ_m and σ_e values versus photon energy were similar to that of μ_m values, as shown in Fig. 3 for sample PEG 200,000. The behavior of σ_a , σ_m and σ_e values for all PEG samples is nearly identical.

The μ_m values, measured and calculated, were used to calculate the effective atomic number (Z_{eff}) and the electron density (N_{eff}) for PEG samples. The Z_{eff} and N_{eff} for PEG 200,000 are listed in Table 2. The percentage differences between the calculation and experimental results are below 1% for the PEG samples (and for other PEG samples) at the designated energies. From Table 2, the Z_{eff} values of PEG lie within the range of the atomic numbers of their constitute elements ($1 < Z_{\text{eff}} < 8$), which is consistent with others findings for low Z constituents' materials [44].

Table 2 Z_{eff} and N_{eff} for PEG 200,000 sample

E (keV)	Measured		Calculated		Percentage difference in Z_{eff} %
	Z_{eff}	N_{eff}	Z_{eff}	N_{eff}	
59.5	3.567 ± 0.091	3.413 ± 0.087	3.580	3.426	0.363
302.9	3.426 ± 0.092	3.278 ± 0.088	3.434	3.285	0.233
356.0	3.414 ± 0.089	3.266 ± 0.085	3.432	3.284	0.524
661.7	3.411 ± 0.093	3.264 ± 0.089	3.430	3.283	0.554
1137.2	3.400 ± 0.090	3.254 ± 0.086	3.429	3.282	0.846
1332.5	3.411 ± 0.091	3.264 ± 0.087	3.430	3.283	0.554

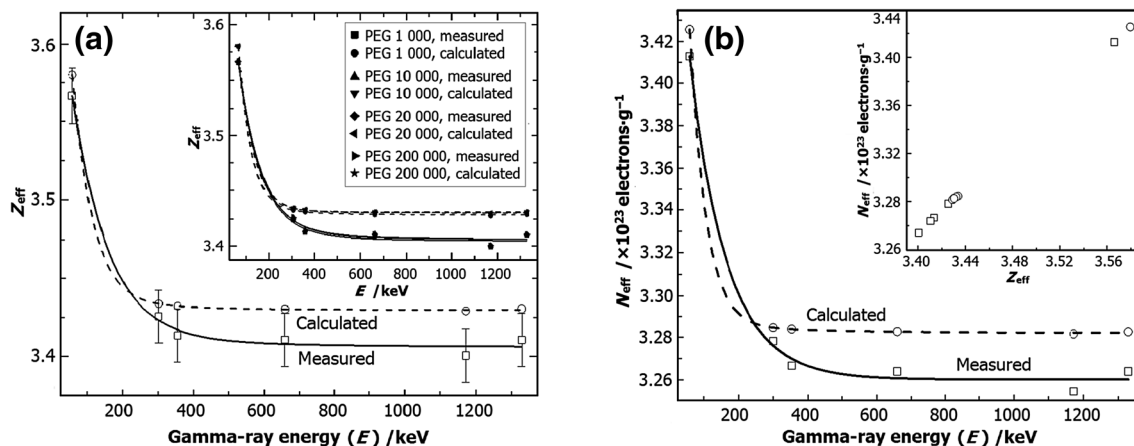


Fig. 4 A typical plot of **a** Z_{eff} and **b** N_{eff} versus photon energy for sample PEG 20,000. The inset in **(b)** shows Z_{eff} versus N_{eff} for sample PEG 20,000. Uncertainty bars indicate the 95% confidence level

The Z_{eff} and N_{eff} versus photon energy for sample PEG 20,000 are shown in Fig. 4, and the inset in Fig. 4a shows the Z_{eff} versus for the other PEG samples. The behavior of Z_{eff} and N_{eff} with energy for all PEG samples is almost the same, and the measurement and calculation results agree well with each other. These confirm that the effective atomic number depends on the energy and interaction processes involved [41]. Although Z_{eff} has its highest value at lower energy region where photoelectric effect is dominant [16], Fig. 4a shows that Z_{eff} values for PEG samples do not vary appreciably over the considered energy range. This observation agrees with the results in Ref. [38] that the effective atomic number tends to remain constant with increasing photon energy in materials containing carbon, hydrogen and oxygen. Also, from the inset in Fig. 4b, N_{eff} increases linearly with Z_{eff} for the PEG samples.

The energy dependence of the HVL values for all PEG samples is given in Table 3. The HVL increases with energy. All PEG samples showed similar behavior, indicating that PEG with various molecular weights is equivalent in attenuating gamma radiation as their HVL values are almost the same.

The variation of theoretical μ_{en}/ρ coefficient and kerma relative to air versus photon energy are given in Table 4 for

all PEG samples. Regarding the values of μ_{en}/ρ coefficient and kerma relative to air, two distinct energy regions are given in Table 4. A strong energy dependence in the low energy region, at which the main interaction mechanism is photoelectric effect, and a less energy dependence in the higher energy regions, at which Compton scattering and pair production processes are the predominant interaction mechanisms.

4 Conclusion

The mass attenuation (μ_{m}) and mass energy-absorption (μ_{en}/ρ) coefficients, total atomic and electronic cross sections (σ_{a} and σ_{e}), half-value layer (HVL), effective atomic (Z_{eff}) and electron (N_{eff}) numbers, and kerma relative to air for PEG in molecular weights of 1000–200,000 have been investigated at 59.5, 302.9, 356.0, 661.7, 1137.2 and 1332.5 keV. The experimental and calculation results agree well with each other. The photon energy and compositional dependence of the values of μ_{m} , σ_{a} and σ_{e} are remarkable in the low energy range due to the predominant photoelectric absorption mechanism. Z_{eff} and N_{eff} behave with photon energy in a similar manner for all PEG

Table 3 Measured (Mea.) and calculated (Cal.) values of *HVL* (cm) for PEG samples of different molecular weights

PEG	59.5 keV		302.9 keV		356.0 keV		661.7 keV		1173.2 keV		1332.5 keV	
	Mea.	Cal.										
1000	2.967 ± 0.078	2.955	4.992 ± 0.128	4.980	5.325 ± 0.135	5.299	6.898 ± 0.175	6.860	9.082 ± 0.230	9.011	9.667 ± 0.245	9.611
10,000	2.968 ± 0.075	2.958	4.993 ± 0.125	4.984	5.326 ± 0.138	5.299	6.899 ± 0.178	6.860	9.086 ± 0.232	9.011	9.671 ± 0.246	9.627
20,000	2.969 ± 0.076	2.958	4.994 ± 0.127	4.984	5.327 ± 0.137	5.299	6.900 ± 0.179	6.860	9.086 ± 0.231	9.011	9.672 ± 0.245	9.627
100,000	2.969 ± 0.075	2.958	4.994 ± 0.128	4.984	5.328 ± 0.139	5.299	6.901 ± 0.172	6.860	9.086 ± 0.233	9.011	9.672 ± 0.244	9.627
200,000	2.969 ± 0.076	2.958	4.994 ± 0.129	4.984	5.328 ± 0.135	5.299	6.901 ± 0.177	6.860	9.086 ± 0.230	9.011	9.672 ± 0.243	9.627

Table 4 Calculated mass energy-absorption energy, μ_{en} (cm²/g), and kerma relative to air for PEG samples of different molecular weights

PEG	59.5 keV		302.9 keV		356.0 keV		661.7 keV		1173.2 keV		1332.5 keV	
	μ_{en}	Kerma										
1000	0.0260	0.8553	0.0313	1.0919	0.0317	1.0922	0.0320	1.0923	0.0296	1.0915	0.0287	1.0923
10,000	0.0295	0.8521	0.0313	1.0916	0.0317	1.0919	0.0320	1.0920	0.0296	1.0912	0.0287	1.0919
20,000	0.0295	0.8519	0.0313	1.0915	0.0317	1.0918	0.0320	1.0920	0.0296	1.0912	0.0287	1.0919
100,000	0.0295	0.8517	0.0313	1.0915	0.0317	1.0918	0.0320	1.0920	0.0296	1.0912	0.0287	1.0919
200,000	0.0295	0.8517	0.0313	1.0915	0.0317	1.0918	0.0320	1.0920	0.0296	1.0912	0.0287	1.0919

samples, and therefore, they were linearly related. *HVL* values increase with photon energy. The energy dependence of μ_{en}/ρ coefficients and kerma relative to air shows two distinct energy regions in which they behave quite differently. To the best of our knowledge, μ_m coefficients and the related radiation energy-absorption parameters of PEG are not available in the literature. Therefore, our results can be useful in scientific and industrial fields of radiation and nuclear physics and chemistry, radiation protection and dosimetry, biomedical and technological applications.

Acknowledgements The authors also thank all members of the Nuclear Science Research Institute at the King Abdulaziz City for Science and Technology in Riyadh, Saudi Arabia, for providing the facilities to conduct the experiments.

References

- I.F. Al-Hamarneh, P.D. Pedrow, S.C. Goheen et al., Impedance spectroscopy study of composite thin films of hydrated polyethylene glycol. *IEEE Trans. Plasma Sci.* **35**, 1518–1526 (2007). doi:[10.1109/tps.2007.906136](https://doi.org/10.1109/tps.2007.906136)
- S.T. Proulx, P. Luciani, A. Christiansen et al., Use of a PEG-conjugated bright near-infrared dye for functional imaging of rerouting of tumor lymphatic drainage after sentinel lymph node metastasis. *Biomaterials* **34**, 5128–5137 (2013). doi:[10.1016/j.biomaterials.2013.03.034](https://doi.org/10.1016/j.biomaterials.2013.03.034)
- I.F. Al-Hamarneh, P.D. Pedrow, A. Eskhan et al., Synthesis and characterization of di(ethylene glycol) vinyl ether films deposited by atmospheric pressure corona discharge plasma. *Surf. Coat. Technol.* **234**, 33–41 (2013). doi:[10.1016/j.surfcoat.2013.06.112](https://doi.org/10.1016/j.surfcoat.2013.06.112)
- M. Zhu, G. Carta, Adsorption of polyethylene-glycolated bovine serum albumin on macroporous and polymer-grafted anion exchangers. *J. Chromatogr. A* **1326**, 29–38 (2014). doi:[10.1016/j.chroma.2013.12.007](https://doi.org/10.1016/j.chroma.2013.12.007)
- F.N. Topchieva, N.V. Efremova, Conjugates of Proteins with Block Co-polymers of Ethylene and Propylene Oxides. *Biotechnol. Genet. Eng. Rev.* **12**, 357–382 (1994). doi:[10.1080/02648725.1994.10647916](https://doi.org/10.1080/02648725.1994.10647916)
- F. Zhang, E.T. Kang, K.G. Neoh et al., Modification of gold surface by grafting of poly(ethylene glycol) for reduction in protein adsorption and platelet adhesion. *J. Biomater. Sci. Polym. E.* **12**, 515–531 (2001). doi:[10.1163/156856201300194252](https://doi.org/10.1163/156856201300194252)
- B. Dong, H. Jiang, S. Manolache et al., Plasma-mediated grafting of poly(ethylene glycol) on polyamide and polyester surfaces and evaluation of antifouling ability of modified substrates. *Langmuir* **23**, 7306–7313 (2007). doi:[10.1021/la0633280](https://doi.org/10.1021/la0633280)
- F.J. Xu, K.G. Neoh, E.T. Kang, Bioactive surfaces and biomaterials via atom transfer radical polymerization. *Prog. Polym. Sci.* **34**, 719–761 (2009). doi:[10.1016/j.progpolymsci.2009.04.005](https://doi.org/10.1016/j.progpolymsci.2009.04.005)
- M.Y. Bai, S.Z. Liu, A simple and general method for preparing antibody-PEG-PLGA sub-micron particles using electrospray technique: an in vitro study of targeted delivery of cisplatin to ovarian cancer cells. *Colloids Surf. B* **117**, 346–353 (2014). doi:[10.1016/j.colsurfb.2014.02.051](https://doi.org/10.1016/j.colsurfb.2014.02.051)
- A. Larsson, T. Ekblad, O. Andersson et al., Photografted poly(ethylene glycol) matrix for affinity interaction studies. *Biomacromolecules* **8**, 287–295 (2007). doi:[10.1021/bm060685g](https://doi.org/10.1021/bm060685g)
- F. Brétagne, H. Rauscher, M. Hasiwa et al., The effect of sterilization processes on the bioadhesive properties and surface chemistry of a plasma-polymerized polyethylene glycol film: XPS characterization and L929 cell proliferation tests. *Acta Biomater.* **4**, 1745–1751 (2008). doi:[10.1016/j.actbio.2008.06.013](https://doi.org/10.1016/j.actbio.2008.06.013)
- F.J. Xu, K.G. Neoh, E.T. Kang, Bioactive surfaces and biomaterials via atom transfer radical polymerization. *Prog. Polym. Sci.* **34**, 719–761 (2009). doi:[10.1016/j.progpolymsci.2009.04.005](https://doi.org/10.1016/j.progpolymsci.2009.04.005)
- S. Zanini, C. Riccardi, E. Grimoldi et al., Plasma-induced graft-polymerization polyethylene glycol acrylate on polypropylene films: chemical characterization and evaluation of the protein adsorption. *J. Colloid Interface Sci.* **341**, 53–58 (2010). doi:[10.1016/j.jcis.2009.09.012](https://doi.org/10.1016/j.jcis.2009.09.012)
- F. Akman, R. Durak, M.F. Turhan et al., Studies on effective atomic numbers, electron densities from mass attenuation coefficients near the K edge in some samarium compounds. *Appl. Radiat. Isot.* **101**, 107–113 (2015). doi:[10.1016/j.apradiso.2015.04.001](https://doi.org/10.1016/j.apradiso.2015.04.001)
- M.I. Sayyed, Investigation of shielding parameters for smart polymers. *Chin. J. Phys.* **54**, 408–415 (2016). doi:[10.1016/j.cjph.2016.05.002](https://doi.org/10.1016/j.cjph.2016.05.002)
- A. Kumar, Studies on effective atomic numbers and electron densities of nucleobases in DNA. *Radiat. Phys. Chem.* **127**, 48–55 (2016). doi:[10.1016/j.radphyschem.2016.06.006](https://doi.org/10.1016/j.radphyschem.2016.06.006)
- T.K. Kumar, K.V. Reddy, Effective atomic numbers for materials of dosimetric interest. *Radiat. Phys. Chem.* **50**, 545–553 (1997). doi:[10.1016/s0969-806x\(97\)00089-3](https://doi.org/10.1016/s0969-806x(97)00089-3)
- N. Koç, H. Özyol, Z-dependence of partial and total photon interactions in some biological samples. *Radiat. Phys. Chem.* **59**, 339–345 (2000). doi:[10.1016/s0969-806x\(00\)00299-1](https://doi.org/10.1016/s0969-806x(00)00299-1)
- N.G. Nayak, M.G. Vijaya, K. Siddappa, Effective atomic numbers of some polymers and other materials for photoelectric process at 59.54 keV. *Radiat. Phys. Chem.* **61**, 559–561 (2001). doi:[10.1016/s0969-806x\(01\)00332-2](https://doi.org/10.1016/s0969-806x(01)00332-2)
- T. Singh, U.Kaur Rajni et al., Photon energy absorption parameters for some polymers. *Ann. Nucl. Energy* **37**, 422–427 (2010). doi:[10.1016/j.anucene.2009.12.017](https://doi.org/10.1016/j.anucene.2009.12.017)
- I. Han, M. Aygun, L. Demir et al., Determination of effective atomic numbers for 3d transition metal alloys with a new semi-empirical approach. *Ann. Nucl. Energy* **39**, 56–61 (2012). doi:[10.1016/j.anucene.2011.09.008](https://doi.org/10.1016/j.anucene.2011.09.008)
- M.W. Marashdeh, I.F. Al-Hamarneh, E.M. Abdel Munem et al., Determining the mass attenuation coefficient, effective atomic number, and electron density of raw wood and binderless particleboards of *Rhizophora* spp. by using Monte Carlo simulation. *Results Phys.* **5**, 228–234 (2015). doi:[10.1016/j.rinp.2015.08.009](https://doi.org/10.1016/j.rinp.2015.08.009)
- M. Kurudirek, Studies on heavy charged particle interaction, water equivalence and Monte Carlo simulation in some gel dosimeters, water, human tissues and water phantoms. *Nucl. Instrum. Methods A* **795**, 239–252 (2015). doi:[10.1016/j.nima.2015.06.001](https://doi.org/10.1016/j.nima.2015.06.001)
- M. Kurudirek, S. Kurudirek, Collisional, radiative and total electron interaction in compound semiconductor detectors and solid state nuclear track detectors: effective atomic number and electron density. *Appl. Radiat. Isot.* **99**, 54–58 (2015). doi:[10.1016/j.apradiso.2015.02.011](https://doi.org/10.1016/j.apradiso.2015.02.011)
- M. Kurudirek, Effective atomic numbers, water and tissue equivalence properties of human tissues, tissue equivalents and dosimetric materials for total electron interaction in the energy region 10 keV–1 GeV. *Appl. Radiat. Isot.* **94**, 1–7 (2014). doi:[10.1016/j.apradiso.2014.07.002](https://doi.org/10.1016/j.apradiso.2014.07.002)
- M. Kurudirek, Effective atomic numbers and electron densities of some human tissues and dosimetric materials for mean energies of various radiation sources relevant to radiotherapy and medical applications. *Radiat. Phys. Chem.* **102**, 139–146 (2014). doi:[10.1016/j.radphyschem.2014.04.033](https://doi.org/10.1016/j.radphyschem.2014.04.033)
- S.R. Benhabbour, H. Sheardown, A. Adronov, Protein resistance of PEG-functionalized dendronized surfaces: effect of PEG

- molecular weight and dendron generation. *Macromolecules* **41**, 4817–4823 (2008). doi:[10.1021/ma8004586](https://doi.org/10.1021/ma8004586)
28. B. Dong, S. Manolache, A.C.L. Wong et al., Antifouling ability of polyethylene glycol of different molecular weights grafted onto polyester surfaces by cold plasma. *Polym. Bull.* **66**, 517–528 (2011). doi:[10.1007/s00289-010-0358-y](https://doi.org/10.1007/s00289-010-0358-y)
29. D. Mech, J.S. Sangwai, Effect of molecular weight of polyethylene glycol (PEG), a hydrate inhibitive water-based drilling fluid additive, on the formation and dissociation kinetics of methane hydrate. *J. Nat. Gas Sci. Eng.* **35**, 1–12 (2016). doi:[10.1016/j.jngse.2016.06.020](https://doi.org/10.1016/j.jngse.2016.06.020)
30. G.C. Lowenthal, P.L. Airey, *Practical Applications of Radioactivity and Nuclear Radiations* (Cambridge University Press, Cambridge, 2001). doi:[10.1017/cbo9780511535376.005](https://doi.org/10.1017/cbo9780511535376.005)
31. J.H. Hubbell, Photon mass attenuation and energy-absorption coefficients. *Int. J. Appl. Radiat. Isot.* **33**, 1269–1290 (1982). doi:[10.1016/0020-708x\(82\)90248-4](https://doi.org/10.1016/0020-708x(82)90248-4)
32. L. Gerward, N. Guilbert, K.B. Jensen et al., WinXCom—a program for calculating x-ray attenuation coefficients. *Radiat. Phys. Chem.* **71**, 653–654 (2004). doi:[10.1016/j.radphyschem.2004.04.040](https://doi.org/10.1016/j.radphyschem.2004.04.040)
33. J.H. Hubbell, S.M. Seltzer, Tables of x-ray mass attenuation coefficients and mass energy-absorption coefficients 1 keV to 20 MeV for elements $Z = 1$ to 92 and 48 additional substances of dosimetric interest. NISTIR-5632 (1995)
34. F. Akman, R. Durak, M.R. Kacal et al., Study of absorption parameters around the K edge for selected compounds of Gd. *X-Ray Spectrom.* **45**, 103–110 (2016). doi:[10.1002/xrs.2676](https://doi.org/10.1002/xrs.2676)
35. Z. Yalçın, O. İçelli, M. Okutan et al., A different perspective to the effective atomic number (Z_{eff}) for some boron compounds and trommel sieve waste (TSW) with a new computer program ZXCOM. *Nucl. Instrum. Methods Phys. Res. A* **686**, 43–47 (2012). doi:[10.1016/j.nima.2012.05.041](https://doi.org/10.1016/j.nima.2012.05.041)
36. M. Taylor, R. Franich, J. Trapp et al., Electron interaction with gel dosimeters: effective atomic numbers for collisional, radiative and total interaction processes. *Radiat. Res.* **171**, 123–126 (2009). doi:[10.1667/rr1438.1](https://doi.org/10.1667/rr1438.1)
37. A. Perumallu, A.N. Rao, G.K. Rao, Photon interaction measurements of certain compounds in the energy range 30–660 keV. *Can. J. Phys.* **62**, 454–459 (1984). doi:[10.1139/p84-064](https://doi.org/10.1139/p84-064)
38. A. El-Kateb, A. Abdul-Hamid, Photon attenuation coefficient study of some materials containing hydrogen, carbon and oxygen. *Int. J. Radiat. Appl. Instrum.* **42**, 303–307 (1991). doi:[10.1016/0883-2889\(91\)90093-g](https://doi.org/10.1016/0883-2889(91)90093-g)
39. K. Singh, H. Singh, V. Sharma et al., Gamma-ray attenuation coefficients in bismuth borate glasses. *Nucl. Instrum. Methods B* **194**, 1–6 (2002). doi:[10.1016/s0168-583x\(02\)00498-6](https://doi.org/10.1016/s0168-583x(02)00498-6)
40. F.H. Attix, *Introduction to Radiological Physics and Radiation Dosimetry* (Wiley, New York, 1986). doi:[10.1002/9783527617135](https://doi.org/10.1002/9783527617135)
41. S.R. Manohara, S.M. Hanagodimath, K.S. Thind et al., On the effective atomic number and electron density: a comprehensive set of formulas for all types of materials and energies above 1 keV. *Nucl. Instrum. Methods B* **266**, 3906–3912 (2008). doi:[10.1016/j.nimb.2008.06.034](https://doi.org/10.1016/j.nimb.2008.06.034)
42. J.H. Hubbell, S.M. Seltzer, Tables of X-Ray Mass Attenuation Coefficients and Mass Energy-Absorption Coefficients (version 1.4). *Radiat. Biomolecular. Phys. Division, PML, NIST* (2004). <http://physics.nist.gov/xaamdi>
43. K.S. Mann, M.S. Heer, A. Rani, Effect of low-Z absorber's thickness on gamma-ray shielding parameters. *Nucl. Instrum. Methods A* **797**, 19–28 (2015). doi:[10.1016/j.nima.2015.06.013](https://doi.org/10.1016/j.nima.2015.06.013)
44. M. Kurudirek, Effective atomic number, energy loss and radiation damage studies in some materials commonly used in nuclear applications for heavy charged particles such as H, C, Mg, Fe, Te, Pb and U. *Radiat. Phys. Chem.* **122**, 15–23 (2016). doi:[10.1016/j.radphyschem.2016.01.012](https://doi.org/10.1016/j.radphyschem.2016.01.012)